Proceedings of Ninth World Conference on Earthquake Engineering
August 2-9, 1988, Tokyo-Kyoto, JAPAN (Vol.II)

3-7-16

EVALUATION OF INTENSITIES OF NEAR-FIELD EARTHQUAKE GROUND MOTIONS BY USING THE EMPIRICAL FORMULA FOR VELOCITY RESPONSE SPECTRA

Masanobu TOHDO[1] and Makoto WATABE[2]

[1]Nuclear Power Division, Toda Construction Co.Ltd.,
Tokyo, Japan
[2]Department of Architecture, University of Tokyo Metropolitan,
Tokyo, Japan

SUMMARY

A method to synthesize earthquake ground motions (EGMs) near a seismic fault is presented. The synthesis is accomplished by superposing the waves radiated from small grid elements. To set the amplitude spectra of element waves, an empirical formula for velocity response spectra is used. Based on this method, peak values and response spectra of near-field EGMs are computed and compared with the ones in 1979 Imperial Valley earthquake. Finally, parametric studies are performed and empirical formulae to predict peak values of near-field EGMs are proposed.

INTRODUCTION

It is well known that active faults can be found anywhere in Japan. Considering the fact in seismic design of structures, it is essential to evaluate the intensities of earthquake ground motions (EGMs), e.g. peak accelerations, at short distances from fault. In EGMs observed at short distances, it has been found the phenomena that peak values in attenuation become flattening, so called saturate (Ref.1). Taking account of the phenomena, formulae based on recorded EGMs to predict peak values had been proposed as shown in Refs.2-4. However, the number of earthquakes in which EGMs near faults had been observed is limited, therefore the prediction by the above formulae may not be adequate. From this point of view, it seems to be necessary that the prediction is complemented by another approach.

Up to the present, the methods with fault model to synthesize EGMs had been proposed (e.g. Refs.5-7). In order to evaluate near-field strong EGMs for engineering purpose, this paper adopts a method similar to the above, in which EGMs due to a large event are synthesized by superposing element waves radiated from subfaults. Our method uses an empirical formula for velocity response spectra in terms of magnitude and distance to set the amplitude spectra of element waves and applies random vibration theory, by which the spectra of synthetic EGMs in far-field fit the empirical formula in a statistical sense.

METHOD TO SYNTHESIZE

Characteristics of Empirical Formula An empirical formula for velocity response spectra, Sv(T) in cm/s, based on the accelerograms recorded at rock sites in Japan were obtained by the authors as follows (Ref.8).

$$\log Sv(M,X,h,T) = 0.607 \cdot M - 1.19 \cdot \log X - 0.85 + g_1(M,T) - g_2(X,T) + g_3(h,M,T) \quad (1)$$

Where T is a period and M, X and h are magnitude, hypocentral distance in km and

critical damping ratio respectively. The functions in the right hand side of Eq. (1) were presented in Ref.8. Here, the constant term of Eq.(1) is modified the spectra so as to represent the ones of EGMs at rock having the shear wave velocity of 0.6km/s-1.0km/s.

The frequency dependent characteristics of Eq.(1) in terms of M and X can be approximately converted into the conventional forms of Eqs.(2) and (3) in the range of M and X of the original used accelerograms.

$$\log Svo(M,T) \propto c(T)\cdot M \tag{2}$$

$$\log Sv(X,T) \propto -b(T)\cdot \log X \tag{3}$$

Where the subscript o indicates response spectra without damping. The results obtained by statistical regression under the uniform distribution of parameters are shown in Fig.1. In addition, if one consider the theoretical form derived from the geometrical spreading of body wave and attenuation by quality factor expressed as

$$\log Sv(X,T) \propto -\log X - b'(T)\cdot X \tag{4}$$

the results become the dotted line in Fig.1. However, the spectra estimated by Eq.(4) have the different trend of attenuation from Eq.(1) as shown in Fig.4.

Superposition Procedure In the synthesis, a main fault with the magnitude of M is divided into small matrix elements (N·N) as shown in Fig.2 which correspond to subfaults with smaller magnitude (Me). For the size of fault, the length (L) and the width (W) can be estimated by Eq.(5) (Refs.9 and 10).

$$\log L \text{ (in km)} = 0.5\cdot M - 1.88, \quad W = L/2 \tag{5}$$

Therefore the scaling factor between main fault and subfault becomes as follows.

$$L/Le = W/We = N = 10^{0.5(M-Me)} \tag{6}$$

The synthesis of an acceleration EGM a(t) at an observatory is accomplished by superposing element waves radiated from each subfault expressed as

$$a(t) = \sum_{i=1}^{N}\sum_{j=1}^{N}\sum_{k=1}^{Nt} a_{eijk}\{t - t_{rij} - (k-1)\tau_{re} - r_{ij}/\beta\} \tag{7}$$

Where N_t is a function with respect to T and is given by Eq.(14). The t_{rij} is the start time of rupture of an element (i,j), ß a shear wave velocity for wave propagation, r_{ij} is shown in Fig.2 and τ_{re} is given by Eq.(8) (Refs.9 and 10).

$$\log \tau_{re} \text{ (in sec.)} = 0.5\cdot Me - 3.03 \tag{8}$$

The element wave is represented by Eq.(9) as nonstationary random process multiplied by envelope function E(t) with the duration time of t_{de}.

$$a_{eijk}(t) = E(t)\cdot a_{sijk}(t) \tag{9}$$

$$E(t) = t/t_m \cdot \exp(1 - t/t_m), \quad t_m = l_e/(2\cdot v_r) + \tau_{re} \tag{10}$$

Where l_e is the length of a subfault in the direction of rupture and v_r is the rupture velocity. Considering the equivalency between Fourier amplitude and velocity response spectrum without damping and the effect of nonstationarity (Ref.11), the stationary process is generated followingly.

$$a_{sijk}(t) = \Sigma_l \; 2/t_{de}\cdot F_{sij}(T_l)\cdot \cos(2\pi/T_l\cdot t + \phi) \tag{11}$$

$$F_{sij}(T) = Svo(Me, r_{eij}, T)/\sqrt{P_E}, \quad P_E = (e/2)^2\cdot t_m/t_{de} \tag{12}$$

Svo(T) in Eq.(12) is obtained by substituting Me, r_{eij} and h=0 into Eq.(1).

In the synthesis of Eq.(7), the phase angles ϕ in Eq.(11) are generated by random number. Consequently, the element waves are uncorrelated each other in terms of i, j and k. In this condition the relationship between $Svo(M,r_c,T)$ of main fault resulting from the synthesis and $Svo(Me,r_c,T)$ under the far-field assumption that is $r_{eij}=r_c=$const. in Eq.(12) can be expressed in the following.

$$\{Svo(M,r_c,T)\}^2 = N^2\cdot N_t\cdot\{Svo(Me,r_c,T)\}^2 \tag{13}$$

Based on this relation, N_t dependent on T is given by Eq.(14) so that the spectrum variation due to M corresponds to the solid line in Fig.1 derived from Eq.(1).

$$\log N_t(T)/N = -(M-Me)\cdot 0.6\cdot\exp(-3T), \quad T;\text{sec.} \tag{14}$$

From the set, N_t becomes 1 in shorter period range. This is similar to the characteristics of theoretical solution on the basis of Haskell's model (Ref.12), in which the term due to source time function becomes irrelevant to source magnitude with higher frequency. In longer period range the spectrum is proportional to 0.75·M because N_t equals N. This result indicates that the EGM synthesized by our method does't keep the seismic moment. Therefore, in the successful synthesis

including period components longer than 5sec., it is necessary to improve our method by considering the effect of correlation among element waves and so on.

In the latter parts, we assume V_r=3km/s, ß=3.5km/s and uni-lateral rupture of fault. For the number of N, the integer is chosen so that Me calculated by Eq. (6) is close to 5.5. For N_t, using an integer near N_t by Eq.(14) the amplitude is corrected by multiplying the square root value of ratio of N_t to the integer. The intensities such as peak values are represented by ensemble average taken across 3 samples of synthesizing. The validity of the synthesis method under the far-field assumption ($r_{eij}=r_c$=50km) is verified through the simulation as shown in Fig.3. From these results it can be seen that the response spectra obtained from synthetic EGMs agree well with the ones calculated by Eq.(1) using M and X=50km.

Synthesis in Near-Field When one synthesize EGMs by substituting Eq.(1) into Eq. (12) with $r_{eij}=X$ which is an actual distance from a point on fault to an observatory, the intensities of EGMs near a fault even in the case of M=5.5 become too large as shown in LX and LN3 lines of Fig.4. This result is caused by higher attenuation with X included in Eq.(1). Accordingly one should take the saturation of wave intensity at short distance even in the smaller event into account. From this point of view, the equivalent distance r_{eij} to determine the amplitude spectra in Eq.(12) is defined in the following.

$$r_{eij}=[\int_0^{Le}\int_0^{We}\{r_m+r(x,y)\}^{-2.5}dx_i dy_j/(Le\cdot We)]^{-1/2.5},\quad r_m=0.75\sqrt{LeWe/\pi} \qquad (15)$$

This definition is based on the consideration that r_{eij} becomes 4km as an observatory is just on a subfault with Me=5.5 (Refs.4 and 13) and the effect of relative situation of an observatory to subfaults divided arbitrarily becomes smaller. The AD-line in Fig.4 is the results synthesized by 1 element using Eq.(15). Then the effect of division of fault plane is examined and the results are shown in Fig.5. In addition the synthetic results by the use of attenuation property expressed by Eq.(4) and in the dotted line of Fig.1 are plotted in Figs.4 and 5 with Q for the first letter, as well. In the case of Q in Fig.5, r_m and the number of 2.5 in Eq. (15) are transformed into 0 and 2, respectively.

APPLICATIONS TO A REAL EARTHQUAKE AND PARAMETRIC STUDIES

Imperial Valley Earthquake, 1979 The locations of the Imperial fault and recording stations are drawn in Fig.6. For the synthesis of 1979 Imperial Valley earthquake (M=6.6), we assume the fault shown in Fig.6 and the fault is divided into 4·4 subfaults with Me=5.4. The amplification effect shown in Fig.7 due to surface layer is also considered. Figures 8 and 9 show peak accelerations and pseudo velocity response spectra due to synthesis respectively, in comparison with the ones by observed accelerograms. From these comparisons it will be recognized that the synthetic results express well the intensities of EGMs due to this earthquake.

Parametric Studies Using the method presented above, parametric studies on peak values are carried out, which have the parameters of M, closest distance to fault (dc) and direction (θ) as shown in Fig.10. The examples of synthetic wave form are traced in Fig.11. The relationships between dc and peak acceleration (A) or peak velocity (V) are plotted in Figs.12 and 13, respectively. On the basis of these studies it is found that empirical formulae to evaluate peak values in near-field can be composed in the following.

$$\log A\ (\text{in Gal}) = 0.440\cdot M-1.38\cdot\log X_A+1.04 \qquad (16)$$

$$\log V\ (\text{in cm/s}) = 0.607\cdot M-1.19\cdot\log X_V-1.40 \qquad (17)$$

Where X_A and X_V with the unit of kilometer are given by

$$X_A = \{(dc+0.6\cdot L^{0.5})^2+(1.4\cdot L^{0.5})^2\}^{1/2} \qquad (18)$$

$$X_V = \{(dc+0.4\cdot L^{0.6})^2+(L^{0.6})^2\}^{1/2} \qquad (19)$$

The solid lines in Figs.12 and 13 are estimated by Eqs.(16) and (17). Figure 14 shows the comparisons among Eq.(16) and other estimations by Refs.3 and 4 with the same set of M and dc in spite of their definitions, together with the plots estimated by tombstone behavior at rock in earthquakes (Ref.14). In the plot due

to Ref.3, peak accelerations are divided by 1.13 in order to compare in the average from 2-components, where Eq.(1) has the same meanings.

CONCLUSIONS

A method to synthesize earthquake ground motions at short distance has been introduced, which has been combined an empirical formula for velocity response spectra with fault model. Based upon the method, simulation analyses for 1979 Imperial Valley earthquake and parametric studies have been performed. Resulting from the studies empirical formulae to estimate peak values have been proposed and it has been evaluated that peak accelerations at rock sites close to the fault with the magnitude of 6.5-7.5 have become 500-600 Gals as average.

REFERENCES

1. Boore,D.M. and Joyner,W.B., "The Empirical Prediction of Ground Motion," Bull. Seism. Soc. Am., 72, S43-S60, (1982).
2. Kanai,K. and Suzuki,T., "Expectancy of the Maximum Velocity Amplitude of Earthquake Motions at Bedrock," Bull. Earthq. Res. Inst., Univ. of Tokyo, XLVI, (1968).
3. Joyner,W.B. and Boore,D.M., "Peak Horizontal Acceleration and Velocity from Strong Motion Records Including Records from the 1979 Imperial Valley, California, Earthquake," Bull. Seism. Soc. Am., 71, 2011-2038, (1981).
4. Campbell,K.W., "Near-Source Attenuation of Peak Horizontal Acceleration," Bull. Seism. Soc. Am., 71, 2039-2070, (1981).
5. Harzell,S., "Earthquake Aftershocks as Green's Functions," Geophys. Res. Letters, 5, 1-4, (1978).
6. Midorikawa,S. and Kobayashi,H., "On Estimation of Strong Earthquake Motions with Regard to Fault Rupture (in Japanese)," Trans. Archi. Inst. Japan, 282, 71-79, (1979).
7. Irikura,K., "Semi-Empirical Estimation of Strong Ground Motions During Large Earthquakes," Bull. Disas. Prev. Res. Inst., Kyoto Univ., 33, 63-104, (1983).
8. Ohsaki,Y., Watabe,M. and Tohdo,M., "Analyses on Seismic Ground Motion Parameters," 7th WCEE, 2, 97-104, (1980).
9. Sato,R., "Theoretical Basis on Relationships between Focal Parameters and Earthquake Magnitude," J. Phys. Earth, 27, 353-372, (1979).
10. Geller,R.J., "Scaling Relations for Earthquake Source Parameters and Magnitude," Bull. Seism. Soc. Am., 66, 1501-1523, (1976).
11. Watabe,M., Iwasaki,R., Tohdo,M. and Ohkawa,I., "Simulation of 3-Dimensional Earthquake Ground Motions along Principal Axes," 7th WCEE, 2, 287-294, (1980).
12. Savage,J.C., "Relation of Corner Frequency to Fault Dimensions," J. Geophys. Res., 77, 3788-3795, (1972).
13. Hadley,D.M., Helmberger,D.V. and Orcutt,J.A., "Peak Acceleration Scaling Studies," Bull. Seism. Soc. Am., 72, 959-979, (1982).
14. Omote,S., Miyake,A. and Narahashi,H., "On Maximum Accelerations in Near-Field (in Japanese)," Annual Meeting of Archi. Inst. Japan, 549-550, (1978).

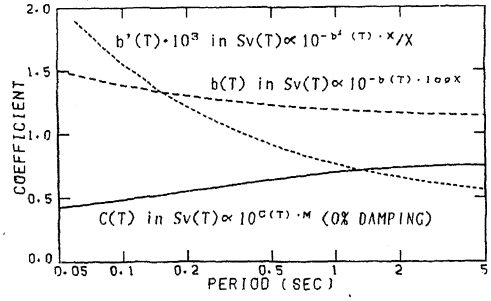

Fig.1 Coefficients Expressing Spectral Characteristics of Empirical Formula for Velocity Response Spectra Sv(T) in Eq.(1)

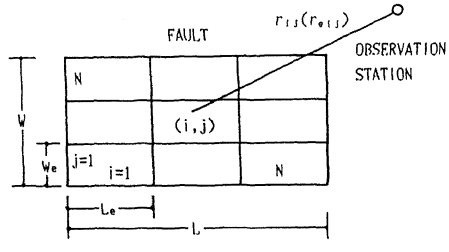

Fig.2 Schematic Views of Main Fault, Subfaults and Observatory for Synthesis

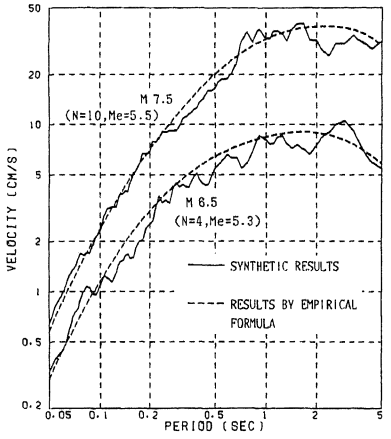

Fig.3 Comparison between Sv(T) with 5% Dampings by the Synthesis under the Far-Field Assumption and the One by Eq.(1)

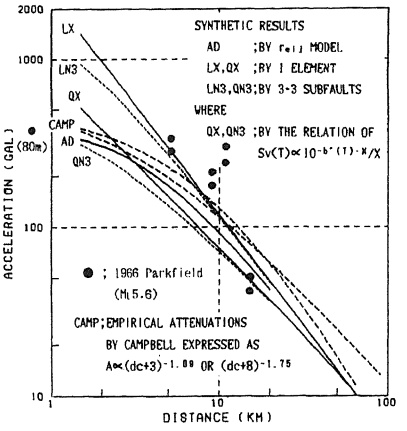

Fig.4 Peak Accelerations due to Various Ways for M=5.5 with Hypocentral Distance for LX, QX and Fault Distance (dc) for the Others

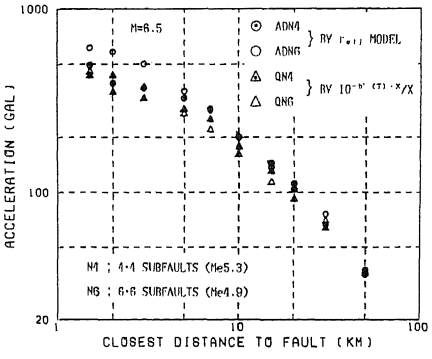

Fig.5 Effects of Number (N) to Divide Fault in Synthesis for M=6.5 (In the following the obervatory is situated at ground surface.)

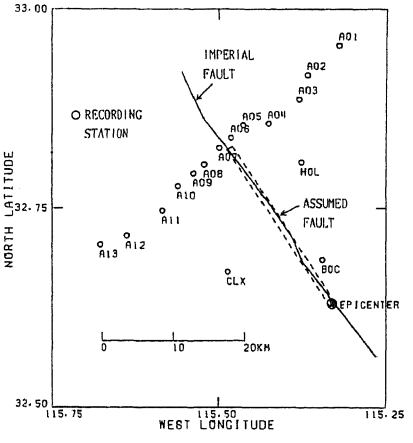

Fig.6 Locations of the Imperial Fault and Recording Stations

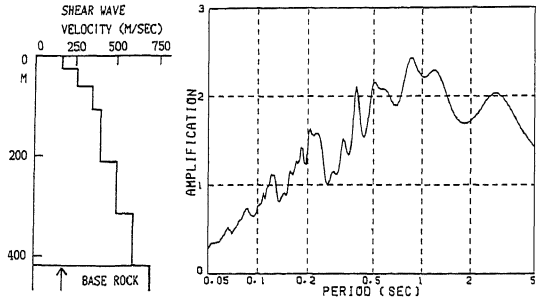

Fig.7 Structure of Soil and Amplification Spectra from Outcropping Base Rock Assumed for Simulation

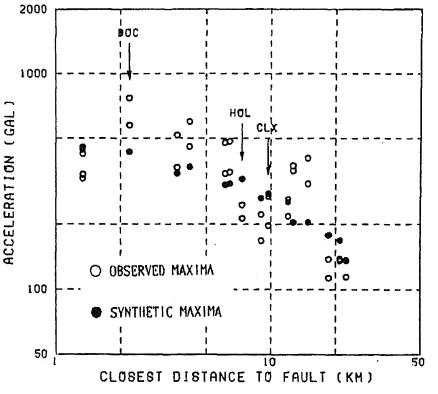

Fig.8 Comparison of Peak Accelerations by Synthesis and Observed Accelerograms

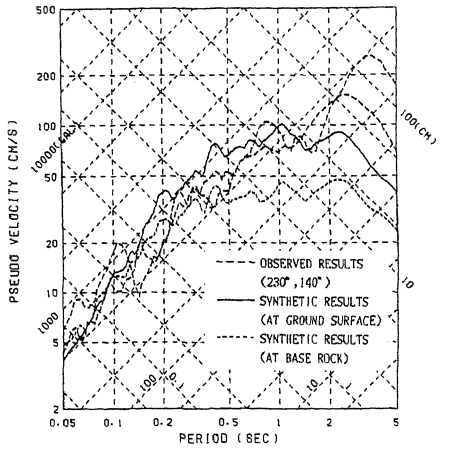

(a) A06 (dc=1.3km)

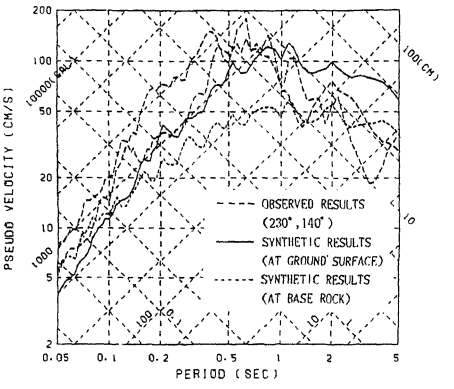

(b) BOC (dc=2.2km)

Fig.9 Comparison of Pseudo Velocity Response Spectra with 5% Dampings for the Imperial Valley Earthquake, 1979

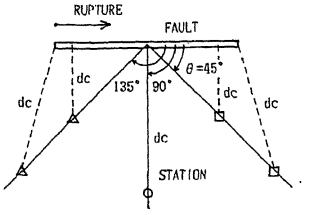

Fig.10 Geometries for Parametric Study

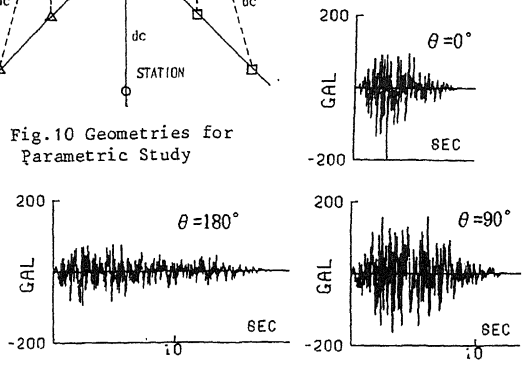

Fig.11 Synthesized Time Histories (M=6.5, dc=L/2)

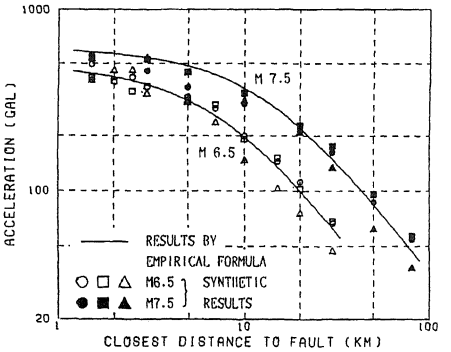

Fig.12 Peak Acceleration versus dc Obtained by Synthesis and Eq.(16)

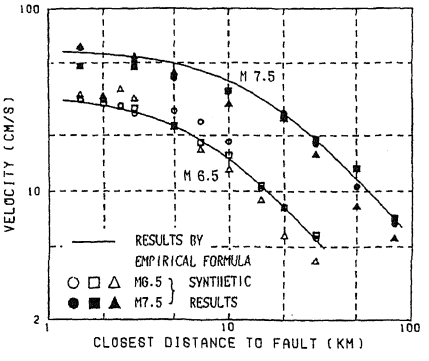

Fig.13 Peak Velocity versus dc Obtained by Synthesis and Eq.(17)

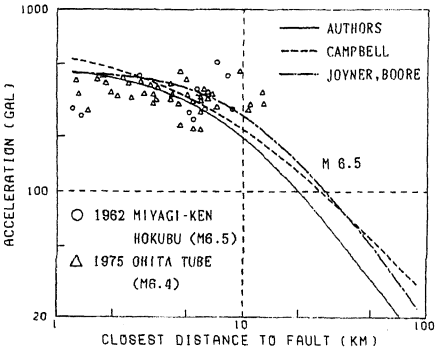

Fig.14 Comparison of Peak Accelerations Estimated by the Authors and Others